Eur Biophys J (2006) 35:647–654
DOI 10.1007/s00249-006-0069-3

ARTICLE

Voltage changes involving photosystem II quinone–iron complex turnover

M. D. Mamedov · A. A. Tyunyatkina · S. A. Siletsky · A. Yu. Semenov

Received: 24 January 2006 / Revised: 10 April 2006 / Accepted: 20 April 2006 / Published online: 18 May 2006

Abstract An electrometrical technique was used to investigate proton-coupled electron transfer between the primary plastoquinone acceptor Q_A^- and the oxidized non-heme iron Fe^{3+} on the acceptor side of photosystem II core particles incorporated into phospholipid vesicles. The sign of the transmembrane electric potential difference $\Delta\psi$ (negative charging of the proteoliposome interior) indicates that the iron–quinone complex faces the interior surface of the proteoliposome membrane. Preoxidation of the non-heme iron was achieved by addition of potassium ferricyanide entrapped into proteoliposomes. Besides the fast unresolvable kinetic phase ($\tau \sim 0.1$ μs) of $\Delta\psi$ generation related to electron transfer between the redox-active tyrosine Y_Z and Q_A, an additional phase in the submillisecond time domain ($\tau \sim 0.1$ ms at 23°C, pH 7.0) and relative amplitude ~ 20% of the amplitude of the fast phase was observed under exposure to the first flash. This phase was absent under the second laser flash, as well as upon the first flash in the presence of DCMU, an inhibitor of electron transfer between Q_A and the secondary quinone Q_B. The rate of the additional electrogenic phase is decreased by about one-half in the presence of D_2O and is reduced with the temperature decrease. On the basis of the above observations we suggest that the submillisecond electrogenic reaction induced by the first flash is due to the vectorial transfer of a proton from external aqueous phase to an amino acid residue(s) in the vicinity of the non-heme iron. The possible role of the non-heme iron in cyclic electron transfer in photosystem II complex is discussed.

Keywords Photosystem II · Proteoliposomes · Non-heme iron · Plastoquinone Q_A · Electron transfer · Transmembrane electric potential difference · An electrometrical technique

Abbreviations

PS II	Photosystem II
RC	Reaction center
WOC	Water-oxidizing complex
P_{680}	Primary electron donor in PS II
Y_Z	Tyrosine 161 on subunit D1 of PS II
Mes	2-(*N*-morpholino)ethanesulfonic acid
Hepes	4-(2-Hydroxyethyl)-1-piperazineethanesulfonic acid
DCMU	3-(3,4-Dichlorophenyl)-1,1-dimethyl urea
Q_A (Q_B)	Primary (secondary) quinone acceptor
Fe^{2+} (Fe^{3+})	Non-heme iron in its reduced (oxidized) state
D1 and D2	Polypeptides consisting the anchoring site of the main cofactors for PS II
$\Delta\psi$	Transmembrane electric potential difference
τ	Characteristic time constant

M. D. Mamedov (✉) · A. A. Tyunyatkina · S. A. Siletsky · A. Yu. Semenov
A.N. Belozersky Institute of Physico-Chemical Biology, Moscow State University, 119992 Moscow, Leninskie Gory, Russia
e-mail: mamedov@genebee.msu.su

A. A. Tyunyatkina
Faculty of Bioengineering and Bioinformatics, Moscow State University, 119992 Moscow, Leninskie Gory, Russia

Introduction

Photosystem II (PS II) is a large pigment–protein complex embedded in the thylakoid membrane of green plants, algae, and cyanobacteria, which functions as a vectorial water-plastoquinone oxidoreductase. The water-oxidizing enzyme complex is coupled to the photosynthetic reaction center (RC) of PS II, a heterodimer of the D1 and D2 polypeptides with general architecture similar to that of the RC of purple bacteria (reviewed in Rutherford et al. 1992; Diner and Babcock 1996; Shinkarev 2004). The three-dimensional structure of PS II has been determined (Ferreira et al. 2004; Loll et al. 2005). The overall process catalyzed by PS II comprises three types of reaction sequences: (a) photooxidation of a chlorophyll *a* special pair (P_{680}) and subsequent stabilization of the primary charge separation by rapid electron transfer from the pheophytin anion to the specially bound plastoquinone (Q_A) (Renger 1992; Diner and Babcock 1996), (b) cooperation of four oxidizing redox equivalents within a manganese-containing functional unit, designated as a water-oxidizing complex (WOC), giving rise to oxidation of two water molecules into dioxygen with release of four protons into the lumen (Debus 1992; Haumann and Junge 1996; Ruttinger and Dismukes 1997; Renger 2004), and (c) reduction of one plastoquinone molecule to plastohydroquinone via a sequence of two single-electron transfer steps with Q_A^- as reductant (Crofts and Wraight 1983; Lavergne and Briantais 1996; Shinkarev 2005).

The inner core of PS II contains two types of iron-containing centers, the heme group(s) of cytochrome b_{559} (Cyt b_{559}) and the non-heme iron located between Q_A and Q_B. In bacterial RC this non-heme iron is coordinated by four histidines, and glutamate (Michel and Deisenhofer 1988), whereas the latter ligand in PS II is substituted by bicarbonate acting as a bidentate ligand (Hienerwadel and Berthomieu 1995; Ferreira et al. 2004). This difference in coordination might be responsible for the markedly lower redox potential of the couple Fe^{3+}/Fe^{2+} in PS II (Petrouleas and Diner 1986; Renger et al. 1987); its pH dependence, –60 mV/pH unit between pH 6.1 and 8.5 indicates the deprotonation of D1His215, an iron ligand located at the Q_B pocket (Berthomieu and Hienerwadel 2001). In PS II, non-heme iron can be oxidized from Fe^{2+} to Fe^{3+} in the dark by addition of potassium ferricyanide (Ikegami and Katoh 1973; Petrouleas and Diner 1986; 1987). Under these conditions, after single excitation of PS II, a non-heme Fe^{3+} is reduced by Q_A^- in submillisecond time domain (Diner et al. 1991; Haumann and Junge 1994) followed by proton uptake probably by amino acid(s) at the stromal side of PS II (Bögershausen and Junge 1995).

Both electron and proton transfer within the PS II complex are either electrogenic or non-electrogenic. Measurements of the electrochromic absorption changes of carotenoids showed that incubation of thylakoids in the presence of potassium ferricyanide leads to appearance of an additional electrogenic phase in the submillisecond time domain (Haumann et al. 1995). This phase can be suppressed by treatment of the thylakoids with DCMU, an inhibitor of electron transfer between Q_A and Q_B. It was suggested that 1/3 of the electrogenicity of Fe^{3+} reduction might be tentatively attributed to electron transfer from Q_A^- to Fe^{3+}, 2/3 to the proton uptake from the stroma (Haumann et al. 1995). However, this suggestion has not been rigorously substantiated by experiment.

The electrogenic nature of the proton-coupled electron transfer reaction between Q_A^- and the non-heme Fe^{3+} was also observed in proteoliposomes containing PS II core complexes (Mamedov et al. 2000).

In the present work, we studied the effect of D_2O and temperature on the kinetics of the proton-coupled electron transfer reaction between Q_A^- and Fe^{3+} in spinach PS II core complexes incorporated into phospholipid vesicles using electrometrical technique. These experiments were intended to clarify the nature of the electrogenic phase coupled to reduction of non-heme iron by Q_A^-.

Materials and methods

All chemicals used were reagents of analytical purity grade. PS II core particles were prepared from market spinach as previously described (Ghanotakis et al. 1987) and resuspended in 20 mM Mes–NaOH buffer (pH 6.5), 15 mM NaCl, 10 mM $CaCl_2$, 5 mM $MgCl_2$, 0.4 M sucrose and 0.03% (w/v) *n*-dodecyl *β*-D-maltoside to chlorophyll concentration of ~ 2.5 mg/ml. The samples were frozen in small aliquots in liquid nitrogen and stored at –80°C until use. Chlorophyll concentration was determined in 80% acetone, according to the method of Porra et al. (1989). The rate of oxygen evolution by the PS II core particles was ~ 1,000–1,200 μmol of O_2 (mg of Chl)$^{-1}$ h^{-1} in the presence of 0.5 mM 2,6-dichloro-*p*-benzoquinone as an electron acceptor.

Mn depletion of the WOC of PS II core particles was performed as described earlier (Ahlbrink et al. 2001) with modifications: 0.8 M Tris buffer, pH 9.0 was added to stock of PS II core particles (concentration of

chlorophyll ~ 0.5 mM) in the ratio 29:1 (v/v) to sediment Mn-depleted PS II core particles by centrifugation (1 h, 31,000 g). The samples were incubated 20 min at room temperature, and then they were pelleted, washed and suspended in assay mixture. After this treatment the rate of oxygen evolution under continuous light illumination was below 5% of that recorded with untreated PS II core particles.

Proteoliposomes with PS II core particles were prepared according to Mamedov et al. (1999). Asolectin (20 mg/ml) from soybean [Sigma, type IV-S, 16% (w/w) phosphatidylcholine content] was dissolved in 50 mM Hepes–NaOH buffer (pH 7.5) containing 0.8% (w/v) *n*-octyl *β*-D-glucopyranoside (Sigma). Protein-free liposomes were prepared by sonication for 3 min using an ultrasonic (UZDN-2T) disintegrator in the pulsed mode at 40 mA, 22 kHz. The clear lipid solution was stored at –80°C until use. Incorporation of the PS II core particles into the liposomes was achieved by mixing of a small volume of samples with liposome suspensions [standard lipid-to-protein ratio of 30 (w/w)] and incubation of the mixture for 30 min at 4°C. After being mixed, the samples were loaded on the Sephadex G50 column (NAP5, Pharmacia). The column was previously equilibrated with 20 mM Hepes–NaOH, pH 7.5 and 5 mM $CaCl_2$. Then samples (0.4–0.5 ml) were collected at a flow rate of 0.9 ml/min employing stepwise elution with 20 mM Hepes–NaOH buffer, pH 7.5 containing 5 mM $CaCl_2$. The proteoliposomes formed were sedimented by centrifugation at 100,000*g* for 1 h and resuspended in the same medium.

When potassium ferricyanide (2 mM) was entrapped into the proteoliposomes, the external ferricyanide was removed from the proteoliposomes by passage through a column of Sephadex G50 with the 20 mM Hepes–NaOH, pH 7.5 and 5 mM $CaCl_2$. Entrapping of ferricyanide molecules into the phospholipid vesicles had minor effect on the orientation of the samples.

Time-resolved electrometric measurements of voltage changes by liposome-reconstituted PS II core particles were carried out as described previously (Semenov et al. 2006). The samples were immobilized in the presence of 10 mM $MgCl_2$ onto one side of a collodion (nitrocellulose) film, impregnated with soybean phosphatidylchloline (~ 100 mg/ml) dissolved in *n*-decane. The film separated the two electrolyte-containing compartments of a dismountable Teflon chamber. After 1 h incubation the unattached samples were removed by volume change providing ~ 40-fold dilution. Saturating light flashes were provided by a frequency-doubled Quantel Nd:YAG laser (wavelength, 532 nm; pulse half-width, 15 ns; flash energy, 30 mJ). The signal was digitized with the aid of the PC-installed Gage 8012 card.

In the case of D_2O experiments, the reading taken from a glass pH electrode, pH_{nom}, deviates from the true pD of D_2O solutions by 0.40 U, so that $pD = pH_{nom} + 0.40$ (Glasoe and Long 1960). We, therefore, corrected the pD in D_2O solutions by adding 0.40 to the nominal reading of our pH meter. Unless indicated otherwise (except Fig. 4) all measurements were performed at 23°C.

The temperature of samples was maintained at a constant level using a thermostatic bath which was connected to a water-jacketed cuvette holder. The temperature was stable within ± 1°C.

The kinetic traces were resolved into individual exponents using the program Discrete (Provencher 1976) and the Microcal Origin 7 software package (Microcal Software).

Results and discussion

Excitation of PS II core particles incorporated into liposomes with a single turnover flash leads to the generation of a $\Delta\psi$ from which the electron transfer rates and dielectrically weighted transmembrane distances between certain redox cofactors can be measured (Semenov et al. 2003). As was shown earlier (Mamedov et al. 1999; 2000), an electrometrically detected flash-induced fast generation of $\Delta\psi$ occurring within the ~ 0.1 μs rise time of the instrument is due to charge separation between the redox-active tyrosine Y_Z of the D1 protein and the primary quinone acceptor Q_A (Fig. 1a). The sign of $\Delta\psi$ (negative charging of the proteoliposome interior) suggests that WOC is facing the outer surface of the membrane, i.e. the polarity of the signal from core particles was opposite to the one obtained with thylakoid membranes (Haumann et al. 1995). The lack of sodium dithionite effect on the amplitude of the voltage change indicates a highly asymmetric orientation of PS II core particles in the liposomes. The slow decay of the voltage change is due to the back reaction from the $S_2Q_A^-$ state (where S_2 is an oxidized form of the Mn cluster); the typical lifetimes are in the order of a few seconds at room temperature (Rappaport et al. 2002). From the relative contribution of the microsecond components in the kinetics of the flash-induced $\Delta\psi$ decay (curve A), we estimate that at least 80% of centers were still active in reducing Y_Z^{ox} by electrons from the WOC.

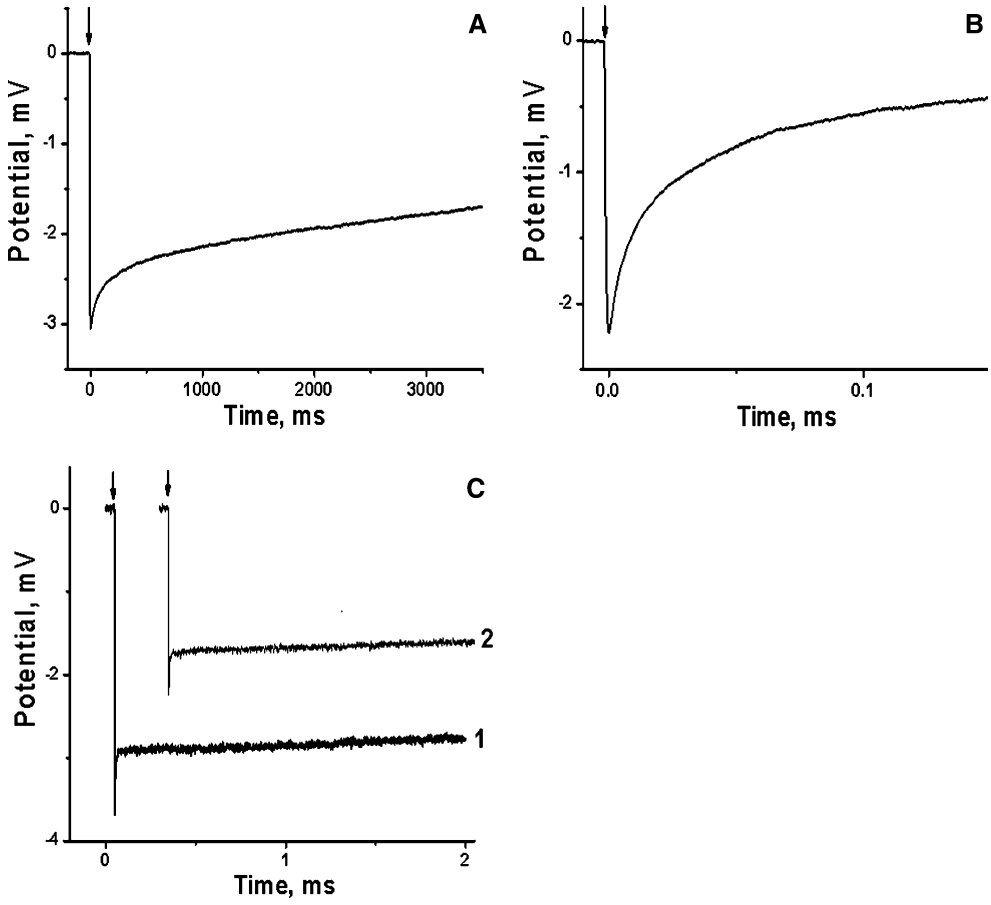

Fig. 1 Voltage changes of proteoliposomes containing PS II core particles with active (**a**) and inactive (**b**) WOC adsorbed onto the phospholipid-impregenated collodion film following the single laser flashes; voltage change of proteoliposomes containing PS II core particles with active WOC following the first (1) and second (2) laser flashes (**c**). The assay mixture contains 20 mM HEPES–NaOH buffer (pH 7.0), 15 mM NaCl, 10 mM $CaCl_2$, 5 mM $MgCl_2$, 0.4 M sucrose, and 1 M glycine betaine. Samples were kept for 10 min in darkness and then excited with laser flash. The dark interval between the first and the second flashes is 1 s. *Arrows* indicate laser flashes

In the liposome-reconstituted PS II core particles with inactive WOC, the photoelectric response decayed more rapidly (curve B) and was attributed to the charge recombination between P^{+}_{680} and Q^{-}_{A} (Gerken et al. 1989; Rappaport and Lavergne 1997).

The PS II core complexes lack Q_B (Ghanotakis et al. 1987). Without external acceptor, the amplitude of the voltage change induced by the first flash was large (curve 1), while voltage changes induced by the second (curve 2) and subsequent (data not shown) flashes were much smaller. This result could be explained as follows: the first flash generates $S_2Q^{-}_{A}$ ($S_2Y_ZP_{680}PheoQ^{-}_{A}$) state, while the subsequent flashes do not induce stable charge separation because Q^{-}_{A} is still present.

Figure 2a shows voltage changes upon the first (curve 1) and second (curve 2) laser flashes in dark-adapted liposome-reconstituted PS II core particles in the presence of 2 mM potassium ferricyanide entrapped into proteoliposomes. The latter procedure causes oxidation of the non-heme iron on the acceptor side of PS II complex (Diner and Petrouleas 1987). Under these conditions, Q^{-}_{A} decayed rapidly between flashes and stable charge separation occurred upon the second flash (curve 2). In addition to the fast phase due to $Y^{ox}_{Z}Q^{-}_{A}$ formation, an additional electrogenic phase in the submillisecond time domain was observed after the first laser flash (curve 1), while this phase was absent in response to the second (curve 2) and subsequent laser flashes (data not shown). The restoration of the additional electrogenic phase in the photoelectric response induced by the first flash (curve 1) was complete after 10 min of dark incubation (data not shown). It is known that the non-heme iron at the acceptor side is oxidized in the time range of minutes (Renger et al. 1987).

The difference between the voltage changes induced by the first and second flashes shown in the inset to Fig. 2a revealed τ of ~ 0.1 ms at pH 7.0. The amplitude of the voltage change related to the non-heme Fe^{3+} reduction by Q^{-}_{A} is ~ 20% of the charge separation $Y^{ox}_{Z}Q^{-}_{A}$ and it is smaller than in thylakoids (~ 30%) measured by electrochromic absorption changes of carotenoids (Haumann et al. 1995). This difference can originate from the use of different sample materials and techniques.

The well known inhibitor of the electron transfer between Q_A and Q_B in PS II, DCMU, added to the incubation medium after 5 min of the dark adaptation

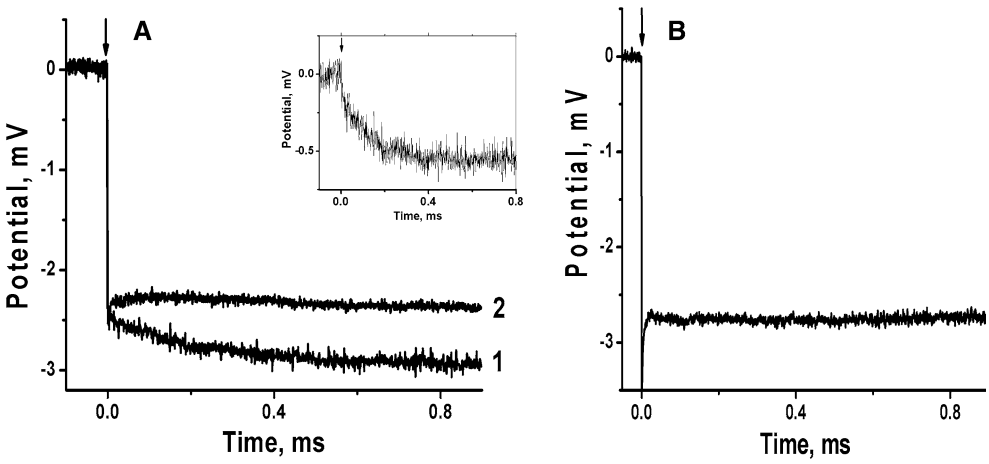

Fig. 2 Voltage changes of proteoliposomes containing oxygen-evolving PS II core particles following the first (1) and second (2) laser flashes in the absence (**a**) and following the first flash in the presence of DCMU (**b**); the difference between traces 1 and 2 is shown on the inset. The experimental conditions as for Fig. 1

had no effect on the $\Delta\psi$ changes induced by light flashes (data not shown). However, when DCMU had been added prior to the dark adaptation, an additional electrogenic phase induced by the first flash was not observed even after 1 h of the incubation (Fig. 2b). The effect of the order of additions of DCMU and ferricyanide is analogous to that reported in Wraight (1985) for fluorescence measurements of Q^{+}_{400}. The lack of an additional electrogenic phase induced by the first flash in the presence of the inhibitor could be explained by 'structural changes' around Q_A, which abolish the ability of its environment to bind protons (Haumann and Junge 1994).

As mentioned above, the reduction of the preoxidized non-heme iron is accompanied by proton uptake (Bögershausen and Junge 1995). Under these conditions, the release of proton induced by the first flash is prevented (Renger et al. 1987).

The kinetics of an additional electrogenic phase revealed in the present work can be approximated by a single exponential component (Fig. 2a, in the inset). This suggests either proximity of electron and H^+ transfer rates under photoinduced Fe^{3+} reduction, or negligible value of one of these components in total electrogenesis.

To study the nature of submillisecond electrogenic component, the kinetics of voltage generation was monitored in the presence of D_2O instead of H_2O (Fig. 3). The rapid phase of the voltage change due to charge separation between Y_Z and Q_A is not affected while an additional electrogenic phase slowed down by a factor of 2.5 ± 0.5 (mean and standard deviation of three measurements). Similar effects were observed for some proton-coupled charge transfer steps in the WOC of PS II (Karge et al. 1997), bacterial RC (Maroti and Wraight 1997) and cytochrome *c* oxidase (Siletsky et al. 2004).

The large value of isotope effect on submillisecond electrogenic component shows that this is caused by the primary kinetics isotope effects, which occur when

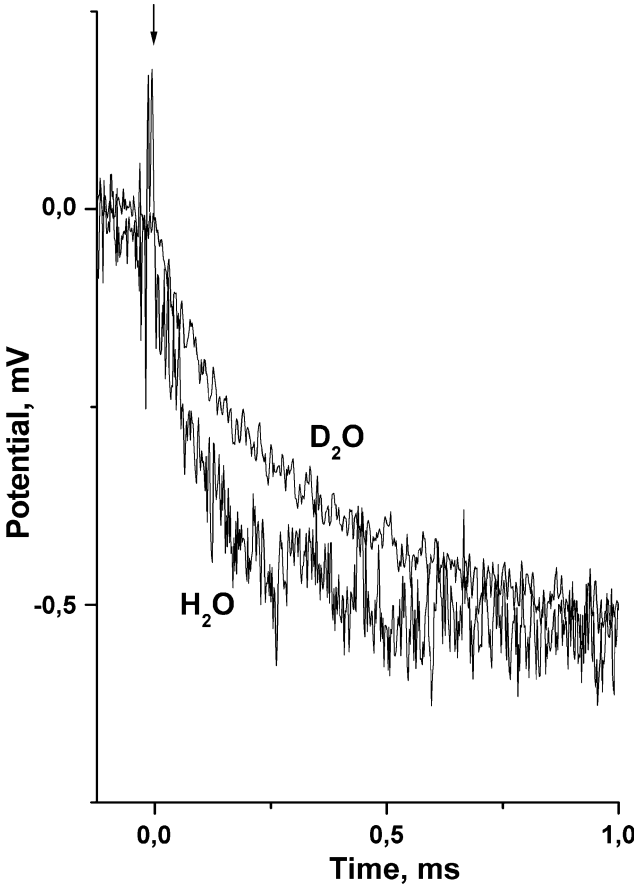

Fig. 3 Effect of H_2O substitution by D_2O on the kinetics of the voltage changes in the oxygen-evolving PS II core complexes. The experiments have been carried out with the same sample of collodion film-adhered liposomes, first recording the response in the H_2O and then replacing it with the D_2O medium. The responses are normalized by the amplitude of the fast electrogenic phase. The experimental conditions as for Fig. 1

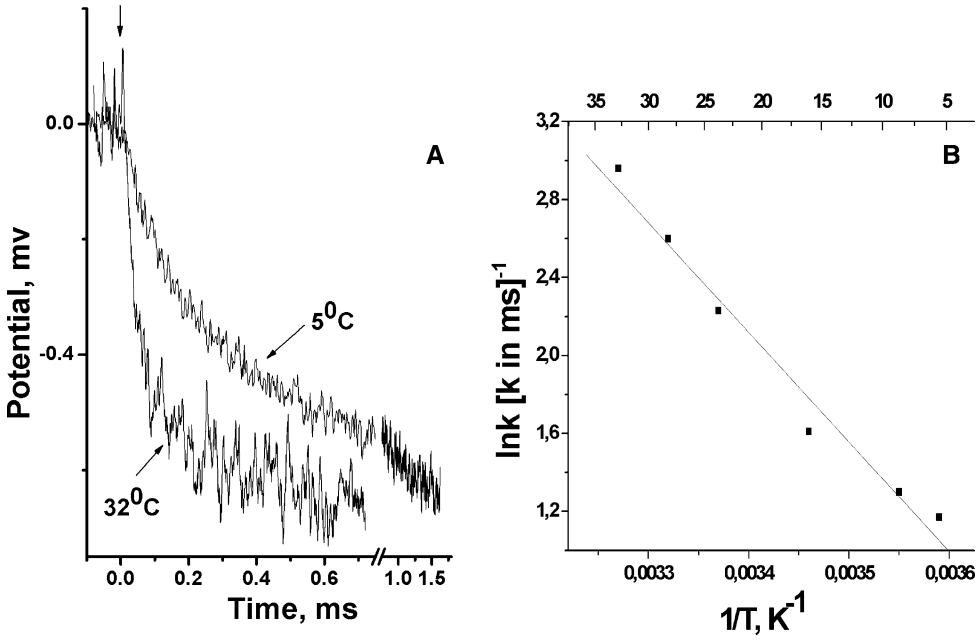

Fig. 4 The flash-induced kinetics of the submillisecond electrogenic phase at 5 and 32°C (**a**). The responses are normalized by the amplitude of the fast electrogenic phase; temperature dependence of the rate constant of additional phase (**b**). The slope of the fit line yielded activation energy E_a of ~ 47 ± 3.5 kJ/mol. The experimental conditions as for Fig. 1

H^+ directly participates in the rate-determining step of the reaction (DeCoursey and Cherny 1997). The secondary isotope effects, which reflect the D^+ for H^+ substitution at some site distinct from the primary reaction site, tend to be smaller (1.02–1.4) (Kirsch 1977). So it is evident that the submillisecond electrogenic component is gated by proton transfer. The X-ray data of PS II core preparations indicate that Q_A and the non-heme iron are located approximately at the same depth with respect to the arbitrary boderline of the lipid bilayer (Ferreira et al. 2004). Thus, the contribution of electron transfer to the total electrogenicity should be negligible. Therefore, we assume that the electrogenic phase accompanying the reduction of Fe^{3+} can be explained by vectorial intraprotein transfer of proton to the putative amino acid at the vicinity of the non-heme iron.

This assumption is further supported by the temperature dependence of the submillisecond electrogenic component. The kinetic traces representing the additional electrogenic phase that is ascribed to proton-coupled electron transfer from Q_A^- to Fe^{3+} at 5 and 32°C are shown in Fig. 4a. A comparison of the traces reveals a significant delay in the kinetics with decreasing temperature. Figure 4b shows the Arrhenius plot of the rate constant of the submillisecond component below + 33°C (pH 7.0). The slope of the fitted line yields activation energy of ~ 47 ± 3.5 kJ/mol.

Similar values of activation energies were observed for light-driven and redox-driven intraprotein proton translocation (Tittor et al. 1989; Gopta et al. 1998; Siletsky et al. 2000). At the same time, the electron transfer reactions that are not coupled to proton transfer have significantly smaller activation energy. Particularly, the $Q_A^-Q_B$ to $Q_AQ_B^-$ electron transfer rate in RCs from *Rhodobacter sphaeroides* has activation energy of ~ 19 kJ/mol (Tiede et al. 1996), while the values of electrogenic reactions attributed to the transfer of the protons fall in the range of 50–60 kJ/mol (Gopta et al. 1998). The values of energy activation for electron (~ 15 kJ/mol) and proton (~ 50–80 kJ/mol) transport were obtained for the cytochrome *c* oxidase (Oliveberg et al. 1989; Siletsky et al. 2000). A value of 54 kJ/mol was found for the M decay of bacteriorhodopsin indicative of the protonation of the Schiff base (Tittor et al. 1989).

It is important to note that high value of activation energy should be attributed to structural changes in the proteins accompanying the intraprotein proton translocation because the proton transfer itself through the continuous network of hydrogen bonds should have relatively small value of activation energy which is close to that of a diffusion-controlled reaction (~ 8–15 kJ/mol) (Maroti and Wraight 1997). Hence, high activation energy is caused by the redox- or light-driven conformational changes of protein structure including the movement of key amino acid residue(s) providing: (a) shift(s) of pK value(s) of proton acceptor group(s) near non-heme iron and/or (b) formation of the continuous intraprotein network or chains of hydrogen bonds in proton-conducting pathway(s) connecting non-heme iron and stroma.

A definitive role of the non-heme iron has yet to be determined. Neither Fe^{2+} nor any divalent cation (Mn^{2+}, Co^{2+}, Ni^{2+}, Cu^{2+} and Zn^{2+}) is required for rapid electron transfer from Q_A^- to Q_B in the bacterial RCs (Debus et al. 1986). However, the presence of a metal ion in the Fe site appears to be necessary for effective electron transfer between Q_A and Q_B (Debus et al. 1986; Remy and Gerwert 2003).

Under physiological conditions, the role of the non-heme iron in electron transfer reactions at the acceptor side of PS II complex is probably of minor relevance because the fast kinetics of water oxidation to molecular oxygen and plastoquinone reduction to plastohydroquinone dominate the reaction pattern. However, under stress conditions affecting the WOC and the Q_B functions, the redox reactions of the non-heme iron probably exert a significant protective function. Assuming that Q_A^- and/or pheophytin ($Pheo^-$) are the electron donors for oxidized Cyt b_{559} (Kaminskaya et al. 2003), the participation of at least one redox mediator group is indispensable for electron transfer from Q_A^- and $Pheo^-$ to Cyt b_{559} at the position determined by X-ray crystallographic structure analysis (Ferreira et al. 2004; Kern et al. 2005). The putative component mediating Cyt b_{559} reduction by photoreduced Q_A^- ($Pheo^-$) could be non-heme iron.

Acknowledgements The authors appreciate the excellent technical assistance of Andrey Zaspa. Thanks are also due to Dr. Chamorovsky S.K. for his valuable discussions. The work was supported by grants from the Russian Foundation for Basic Research (04-04-49441; 06-04-48672, 06-04-48608), grants from International Science and Technology Center (2296) and Russian Federal Agency for Science and Innovation (2005 ZhS-12.5/003).

References

Ahlbrink R, Semin BK, Mulkidjanian AY, Junge W (2001) Photosystem II of peas: effects of added divalent cations of Mn, Fe, Mg, and Ca on two kinetic components of $P680^+$ reduction in Mn-depleted core particles. Biochim Biophys Acta 1506:117–126

Berthomieu C, Hienerwadel R (2001) Iron coordination in photosystem II: interaction between bicarbonate and the Q_B pocket studied by Fourier transform infrared spectroscopy. Biochemistry 40:4044–4052

Bögershausen O, Junge W (1995) Rapid proton transfer under flashing light at both functional sides of dark-adapted photosystem II particles. Biochim Biophys Acta 1230:177–185

Crofts AR, Wraight CA (1983) The electrochemical domain of photosynthesis. Biochim Biophys Acta 726:149–185

Debus R (1992) The manganese and calcium ions of photosynthetic oxygen evolution. Biochim Biophys Acta 1102:269–352

Debus RJ, Feher G, Okamura MY (1986) Iron-depleted reaction centers from *Rhodopseudomas sphaeroides* R-26.1: characterization and reconstitution with Fe^{2+}, Mn^{2+}, Co^{2+}, Cu^{2+}, and Zn^{2+}. Biochemistry 25:2276–2287

DeCoursey TE, Cherny VV (1997) Deuterium isotope effects on permeation and gating of proton channels in rat alveolar epithelium. J Gen Physiol 109:415–434

Diner BA, Babcock GT (1996) In: Ort DR, Yocum CF (eds) Oxygenic photosynthesis: the light reactions. Kluwer, Dordrecht, pp 213–247

Diner BA, Petrouleas V (1987) Light-induced oxidation of the acceptor side Fe(II) of photosystem II by exogenous quinones acting through the Q_B binding site II. Blockage by inhibitors and their effects on the Fe(III) EPR spectra. Biochim Biophys Acta 893:138–148

Diner BA, Petrouleas V, Wendoloski JJ (1991) The iron–quinone electron-acceptor complex of photosystem II. Physiol Plant 81:423–436

Ferreira KN, Iverson TM, Maghlaoui K, Barber J, Iwata S (2004) Architecture of the photosynthetic oxygen-evolving center. Science 303:1831–1838

Gerken S, Dekker JP, Schlodder E, Witt HT (1989) Studies on the multiphasic charge recombination between chlorophyll a^+_{II} ($P\text{-}680^+$) and plastoquinone Q_A^- in photosystem II complexes. Ultraviolet difference spectrum of Chl-a^+_{II}/Chl-a_{II}. Biochim Biophys Acta 977:52–61

Ghanotakis DF, Demetriou DM, Yocum CF (1987) Isolation and characterization of an oxygen-evolving photosystem II reaction center core preparation and a 28 kDa chl-a-binding protein. Biochim Biophys Acta 891:15–21

Glasoe PK, Long FA (1960) Use of glass electrodes to measure acidities in deuterium oxide. J Phys Chem 64:188–190

Gopta OA, Cherepanov DA, Mulkidjanian AY, Semenov AYu, Block DA (1998) Effect of temperature and surface potential on the electrogenic proton uptake in the Q_B site of the *Rhodobacter sphaeroides* photosynthetic reaction center: $Q_A^-Q_B \rightarrow Q_AQ_BH_2$. Photosynth Res 55:309–316

Haumann M, Junge W (1994) The rates of proton uptake and electron transfer at the reducing side of photosystem II in thylakoids. FEBS Lett 347:45–50

Haumann M, Junge W (1996) In: Ort DR, Yocum CF (eds) Oxygenic photosynthesis: the light reactions. Kluwer, Dordrecht, pp 165–192

Haumann M, Hundelt M, Drevenstedt W, Junge W (1995) In: Mathis P (ed) Photosynthesis: from light to biosphere. Kluwer, Dordrecht, pp 333–336

Hienerwadel R, Berthomieu C (1995) Bicarbonate binding to the non-heme iron of photosystem II investigated by Fourier transform infrared difference spectroscopy and 13C-labelled bicarbonate. Biochemistry 34:16288–16297

Ikegami I, Katoh S (1973) Studies on chlorophyll fluorescence in chloroplasts. II. Effect of ferricyanide on induction of fluorescence in presene of 3-(3,4-dichlorophenyl)-1,1-dimethylurea. Plant Cell Physiol 14:829–836

Kaminskaya O, Renger G, Shuvalov VA (2003) Effect of dehydration on light-induced reactions in photosystem II: photoreactions of cytochrome b559. Biochemistry 42:8119–8132

Karge M, Irrgang K-D, Renger G (1997) Analysis of the reaction coordinate of photosynthetic water oxidation by kinetic measurements of 355 nm absorption changes at different temperatures in photosystem II preparations suspended in either H_2O or D_2O. Biochemistry 36:8904–8913

Kern J, Loll B, Zouni A, Saenger W, Irrgang K-D, Biesiadka J (2005) Cyanobacterial photosystem II at 3.2 Å resolution—the plastoquinone binding pockets. Photosynth Res 84:153–159

Kirsch JF (1977) Secondary kinetic isotope effects. In: Cleland WW, O'Leary MH, Northrop DB (eds) Isotope effects on enzyme-catalyzed reactions. University Park Press, Baltimore, pp 100–121

Lavergne J, Briantais JM (1996) Photosystem II heterogeneity. In: Ort DR, Yocum CY (eds) Oxygenic photosynthesis: the light reactions. Kluwer, Dordrecht, pp 265–287

Loll B, Kern J, Saenger W, Zouni F, Biesiadka J (2005) Towards complete cofactor arrangement in the 3.0 Å resolution structure of photosystem II. Nature 438:1040–1044

Mamedov MD, Beshta OE, Gourovskaya KN, Mamedova AA, Neverov KD, Samuilov VD, Semenov AY (1999) Photoelectric responses of the photosystem II oxygen-evolving complexes. Biochemistry (Moscow) 64:606–611

Mamedov MD, Beshta OE, Shutilova NI, Semenov AYu, Samuilov VD (2000) Photoelectric response generated under non-heme iron reduction on the photosystem II acceptor side. Biochemistry (Moscow) 65:728–731

Maroti P, Wraight CA (1997) Kinetics of H^+ ion binding by the $P^+Q_A^-$ state of biochemical photosynthetic reaction centers: rate limitation within the protein. Biophys J 73:367–381

Michel H, Deisenhofer J (1988) Relevance of the photosynthetic reaction center from purple bacteria to the structure of photosystem II. Biochemistry 27:1–7

Oliveberg M, Brzezinski P, Malmstrom BG (1989) The effect of pH and temperature on the reaction of fully reduced and mixed-valence cytochrome *c* oxidase with dioxygen. Biochim Biophys Acta 977:322–328

Petrouleas V, Diner BA (1986) Identification of Q_{400}, a high-potential electron acceptor of photosystem II, with the iron of the quinone–iron acceptor complex. Biochim Biophys Acta 849:264–275

Petrouleas V, Diner BA (1987) Light-induced oxidation of the acceptor side Fe(II) of photosystem II by exogenous quinones acting through the Q_B binding site. I. Quinones, kinetics and pH-dependence. Biochim Biophys Acta 893:126–137

Porra RJ, Thompson WA, Kriedmann PE (1989) Determination of accurate extinction coefficients and simultaneous equations for assaying chlorophylls and extracted with four different solvents: verification of the concentrations of chlorophyll standards by absorption spectroscopy. Biochim Biophys Acta 975:384–394

Provencher SW (1976) A Fourier method for the analysis of experimental decay curves. Biophys J 16:27–41

Rappaport F, Lavergne J (1997) Charge recombination and proton transfer in manganese-depleted photosystem II. Biochemistry 36:15294–15302

Rappaport F, Guergova-Kuras M, Nixon PJ, Diner BA, Lavergne J (2002) Kinetics and pathways of charge recombination in photosystem II. Biochemistry 41:8518–8527

Remy A, Gerwert K (2003) Coupling of light-induced electron transfer to proton uptake in photosynthesis. Nat Struct Biol 10:637–644

Renger G (1992) Energy transfer and trapping in photosystem II. In: Barber J (ed) The photosystems: structure, function and molecular biology. Elsevier, Amsterdam, pp 45–99

Renger G (2004) Coupling of electron and proton transfer in oxidative water cleavage in photosynthesis. Biochim Biophys Acta 1655:195–204

Renger G, Wacker U, Volker M (1987) Studies on the protolytic reactions coupled with water cleavage in photosystem II membrane fragments. Photosynth Res 13:167–184

Rutherford AW, Zimmerman JL, Boussac A (1992) Oxygen evolution. Top Photosynth 11:179–229

Ruttinger W, Dismukes GC (1997) Synthetic water-oxidation catalysts for artificial photosynthetic water oxidation. Chem Rev 97:1–24

Semenov AYu, Mamedov MD, Chamorovsky SK (2003) Photoelectric studies of the transmembrane charge transfer reactions in photosystem I pigment–protein complexes. FEBS Lett 553:223–228

Semenov AYu, Mamedov MD, Chamorovsky SK (2006) Electrogenic reactions associated with electron transfer in photosystem I. In: Golbeck JH (ed) Advances in photosynthesis and respiration. Series Photosystem I: the light-driven, platocyanin:ferredoxin oxidoreductase, chap 21. Kluwer, Dordrecht, pp 319–424

Shinkarev VP (2004) Chlorophyll fluorescence: a signature of photosynthesis. In: Papageorgiou GC, Govindjee (eds) Photosystem II: oxygen evolution and chlorophyll a fluorescence induced by multiple flashes, chap 8. Kluwer, Dordrecht, pp 197–229

Shinkarev VP (2005) Flash-induced oxygen evolution and other oscillation processes in photosystem II. In: Wydrzynski T, Satoh K (eds) Photosystem II: the water/plastoquinone oxido-reductase in photosynthesis, chap 24. Kluwer, Dordrecht

Siletsky S, Zaslavsky D, Smirnova I, Kaulen A, Konstantinov A (2000) F-to-O transition of cytochrome *c* oxidase: pH and temperature effects on the kinetics of charge translocation. Abstracts of the 18th International Congress of Biochemistry and Molecular Biology, Birmingham, p 457

Siletsky SA, Pawate AS, Weiss K, Gennis RB, Konstantinov AA (2004) Transmembrane charge separation during the ferryl-oxo $\rightarrow$ oxidized transition in a nonpumping mutant of cytochrome *c* oxidase. J Biol Chem 279:52558–52565

Tiede DM, Vazquez J, Cordova J, Marone PA (1996) Time-resolved electrochromism associated with the formation of quinone anions in the *Rhodobacter sphaeroides* R26 reaction center. Biochemistry 35:10763–10775

Tittor J, Soell C, Oesterhelt D, Butt H-J, Bamberg E (1989) A defective proton pump, point-mutated bacteriorhodopsin Asp96 $\rightarrow$ Asn is fully reactivated by azide. EMBO J 8:3477–3482

Wraight CA (1985) Modulation of herbicide-binding by the redox state of Q_{400}, an endogenous component of photosystem II. Biochim Biophys Acta 809:320–330